
AVALANCHES IN THE DIRECTED PERCOLATION DEPINNING AND SELF-ORGANIZED DEPINNING MODELS OF INTERFACE ROUGHENING

S. V. BULDYREV*, L. A. N. AMARAL*, A.-L. BARABÁSI*,
S. T. HARRINGTON*, S. HAVLIN*[†], J. KERTÉSZ[‡],
R. SADR-LAHIJANY* and H. E. STANLEY*

**Center for Polymer Studies and Department of Physics,
Boston University, Boston, MA 02215 USA*

[†]Minerva Center and Department of Physics, Bar-Ilan University, Ramat Gan, Israel

[‡]Institute of Physics, Technical University, Budapest, Budafoki ut 8, H-1111, Hungary

Abstract

We review the recently introduced Directed Percolation Depinning (DPD) and Self-Organized Depinning (SOD) models for interface roughening with quenched disorder. The differences in the dynamics of the invasion process in these two models are discussed and different avalanche definitions are presented. The scaling properties of the avalanche size distribution and the properties of active cells are discussed.

1. INTRODUCTION

Recently the growth of rough interfaces has witnessed an explosion of theoretical, numerical, and experimental studies, fueled by the broad interdisciplinary aspects of the subject.^{1–6} Applications can be as diverse as imbibition in porous media, fluid–fluid displacement, bacterial colony growth, fire front motion, and the motion of flux lines in superconductors.^{7–18}

In general, a d -dimensional self-affine interface, described by a single-valued function $h(x, t)$, evolves in a $(d + 1)$ -dimensional medium. Usually some form of disorder η affects

the motion of the interface leading to its roughening. Two main classes of disorder have been discussed in the literature. The first, called thermal or “annealed”, depends only on time. The second, referred to as “quenched”, is frozen in the medium. Early studies focused on time-dependent uncorrelated disorder as being responsible for the roughening. Here, we focus on the effect of quenched disorder on the growth.

The roughening process can be quantified by studying the *global* interface width W :

$$W(L, t) \equiv \langle (\overline{h^2(x, t)} - \overline{h(x, t)}^2)^{1/2} \rangle, \quad (1.1)$$

where L is the system size, the bar denotes a spatial average, and the brackets denote an average over realizations of the disorder. The study of discrete models^{19–22} and continuum growth equations^{23,24} leads to the observation that during the initial period of the growth, i.e., for $t \ll t_\times(L)$, the width grows with time as:

$$W(t) \sim t^\beta \quad [t \ll t_\times], \quad (1.2)$$

where β is the *growth* exponent. For times much larger than t_\times , the width saturates to a constant value. It was observed that the saturation width of the interface W_{sat} scales with L as:

$$W_{sat} \sim L^\alpha \quad [t \gg t_\times], \quad (1.3)$$

where α is the *roughness* exponent. The dependence of t_\times on L allows the combination of Eqs. (1.2) and (1.3) into a single scaling law¹⁹:

$$W(L, t) \sim L^\alpha f_1(t/t_\times), \quad (1.4a)$$

where

$$t_\times \sim L^z. \quad (1.4b)$$

Here $z = \alpha/\beta$ is the *dynamical* exponent, and $f_1(u)$ is a universal scaling function that grows as u^β when $u \ll 1$, and approaches a constant when $u \gg 1$.

An alternative way of determining the scaling exponents is to study the *local* width w in an observation window of length $\ell < L$. The scaling law [Eq. (1.4)], and the fact that the interface is self-affine, allow us to conclude:

$$w(\ell, t) \sim \ell^\alpha f_2(\ell/\ell_\times), \quad (1.5a)$$

where

$$\ell_\times \sim t^{1/z} \quad [t \ll t_\times], \quad (1.5b)$$

or

$$\ell_\times \sim L \quad [t \gg t_\times]. \quad (1.5c)$$

Here $f_2(u)$ is a universal scaling function that decreases as $u^{-\alpha}$ when $u \gg 1$ and approaches a constant when $u \ll 1$.

The simulation of discrete models^{19–22} gives exponents that agree with the predictions of phenomenological continuum approaches, such as the Edwards-Wilkinson (EW) equation²³ and the Kardar-Parisi-Zhang (KPZ) equation.²⁴ However, experimental studies find exponents significantly larger than the predictions of theory, e.g., for (1+1) dimensions, Refs. 23 and 24 predict $\alpha = 1/2$ but experiments show $\alpha \sim 0.6 - 1.0$.^{7–18} Although various explanations have been proposed — long-range correlations,²⁵ power-law distribution²⁶ for the

disorder, or coupling of the interface to impurities²⁷ — it is currently accepted that *quenched* disorder plays an essential role in those experiments.^{13–18,28,30–38,40–44}

The presence of quenched disorder allows an interesting analogy with critical phenomena. The continual motion of the interface requires the application of a driving force F . There exists a critical value F_c such that for $F < F_c$, the interface will become pinned by the disorder after some finite time. For $F > F_c$, the interface moves indefinitely with a constant velocity v . This means that the motion of driven rough interfaces in disordered media can be studied as a phase transition — called the depinning transition. The velocity of the interface v plays the role of the *order parameter*, since as $F \rightarrow F_c^+$, v vanishes as:

$$v \sim f^\theta, \quad (1.6)$$

where θ is the *velocity* exponent, and $f \equiv (F - F_c)/F_c$ is the *reduced force*.

For $F \rightarrow F_c^+$, large but finite regions of the interface are pinned by the disorder. Near the transition, the characteristic length ξ of these pinned regions diverges,

$$\xi \sim f^{-\nu}, \quad (1.7)$$

where ν is the *correlation length* exponent.

Several models in which quenched disorder plays an essential role have been proposed recently.^{13–18,28,30–44} For one class of models,^{13,14,28,40} in $(1 + 1)$ dimensions, α can be obtained by mapping the interface, at the depinning transition onto *Directed Percolation* (DP). In higher dimensions the interface can be mapped to *Directed Surfaces* (DS).¹⁶ In $(1 + 1)$ dimensions, DP and DS are equivalent. We refer to this class of models as the *Directed Percolation Depinning* (DPD) universality class.

Recent numerical studies,⁴⁰ supported by analytical arguments,⁴¹ showed that this class of models can be described by a stochastic differential equation of the KPZ type³⁸:

$$\frac{\partial h}{\partial t} = F + \nabla^2 h + \lambda(\nabla h)^2 + \eta(x, h), \quad (1.8)$$

where $\eta(x, h)$ represents the quenched disorder, and the coefficient λ of the nonlinear term diverges at the depinning transition.⁴⁰ This equation was originally proposed in the context of interface roughening in the presence of quenched disorder in Ref. 38. The numerical integration of Eq. (1.8) yielded exponents in agreement with the calculations for the models in the DPD universality class.³⁸ A recent attempt³⁹ at using a renormalization group approach for Eq. (1.8) suggests that there is a strong coupling fixed point at which the coupling constant associated with the KPZ nonlinearity diverges at the threshold, which is in agreement with Ref. 40. Hence, the high-dimensional behavior of Eq. (1.8) remains an unsolved problem. For a number of different models^{30–35,42} belonging to a second universality class — referred to as *isotropic growth* models — we have either $\lambda = 0$ or $\lambda \rightarrow 0$ at the depinning transition.⁴⁰ Therefore, near the depinning transition, they can be described by an equation of the EW type with quenched disorder⁴⁵:

$$\frac{\partial h}{\partial t} = F + \nabla^2 h + \eta(x, h). \quad (1.9)$$

This equation has been studied by means of the functional renormalization group,^{43,44} yielding $\alpha = \epsilon/3$, $\nu = 1/(2 - \alpha)$, and $z = 2 - 2\epsilon/9$, where $\epsilon = 4 - d$. Thus the upper critical dimension for Eq. (1.9) is 4. When $F \gg F_c$, the size of the pinned regions in the interface

ξ decreases to values much smaller than the system size L . For length scales ℓ larger than ξ , the quenched disorder becomes irrelevant and time-dependent noise dominates the roughening process. This means that for $\ell \ll \xi$, we should recover the results of either the EW or the KPZ equation with annealed noise (depending on the absence or presence of nonlinear terms). This behavior has been observed in some of the experiments⁷⁻¹² and in simulations of discrete models.^{13-16,28,30-35,42}

Theoretical interest in the behavior of Eq. (1.8) in high dimensions motivated the investigation of the DPD problem on the Cayley Tree,⁴⁶ which is usually believed to describe the infinite dimensional limit of the system. The exact solution on the Cayley Tree yields $\alpha = 0$ and suggests that the upper critical dimension is infinity, the conclusion being supported by numerical simulations.⁴⁷ The roughness exponent α remains positive for every finite dimension similar to the original KPZ equation, but unlike Eq. (1.9), in which $\alpha = 0$ at $d \geq 4$. However, recent numerical results⁴⁸ support the latter conclusion. The relation between Eqs. (18) and (19) and the DPD model is also discussed in Ref. 49. The numerical and theoretical results of Refs. 48 and 49 reveal small but significant discrepancies compared with Ref. 47 which await further investigation.

The DPD model, discussed in this paper, was introduced in Refs. 13 and 14 to explain a set of simple imbibition experiments — a somewhat different model, belonging to the same universality class, was independently introduced by Tang and Leschhorn.²⁸ In these experiments a colored suspension (coffee or ink) imbibes a sheet of paper, in the $(1+1)$ -dimensional case — or a porous, spongy-like brick, in the $(2+1)$ -dimensional case.¹³⁻¹⁸ The experimentally measured roughness exponents are in good agreement with the predictions of the DPD models.^{13-16,28} However, a number of experimental features cannot be explained by this model²⁹ (See also Ref. 11). For example, in the experiments, the saturation width and the average height of the pinned interface depend on the rate of evaporation, which is not taken into account in the DPD model. A variant of the DPD model that explains the experimental results in terms of the effect of evaporation is discussed in Ref. 18.

A self-organized variant of the DPD model has been introduced by Havlin et al.¹³ who used the analogy with invasion percolation. Similar model was studied by Sneppen and others.⁵⁰ We will call these models the models of Self-Organized Depinning (SOD). In these models growth proceeds by avalanches, whose properties are of interest not only for the study of interface roughening,⁵⁰⁻⁵³ but also for other fields, including biological evolution in ecological systems.⁵⁴⁻⁵⁷ In this paper we will address some open questions concerning static and dynamic properties of the DPD and SOD models.

2. AVALANCHES IN DPD AND SOD MODELS

In both the DPD and SOD models the fluid interface propagates in a lattice with quenched disorder. Each cell on the lattice has a pinning threshold η_i that is uniformly distributed between 0 and 1. However, the rules of update in these models are different. The question is: What are the similarities and the differences in the dynamics of these models?

In the DPD model, at each time step, each dry cell that is a nearest-neighbor to a wet cell becomes wet if its threshold η_i is less than the value of a driving force p . In addition, there is a rule of erosion of overhangs: all the cells that are below a wet cell become wet instantaneously.

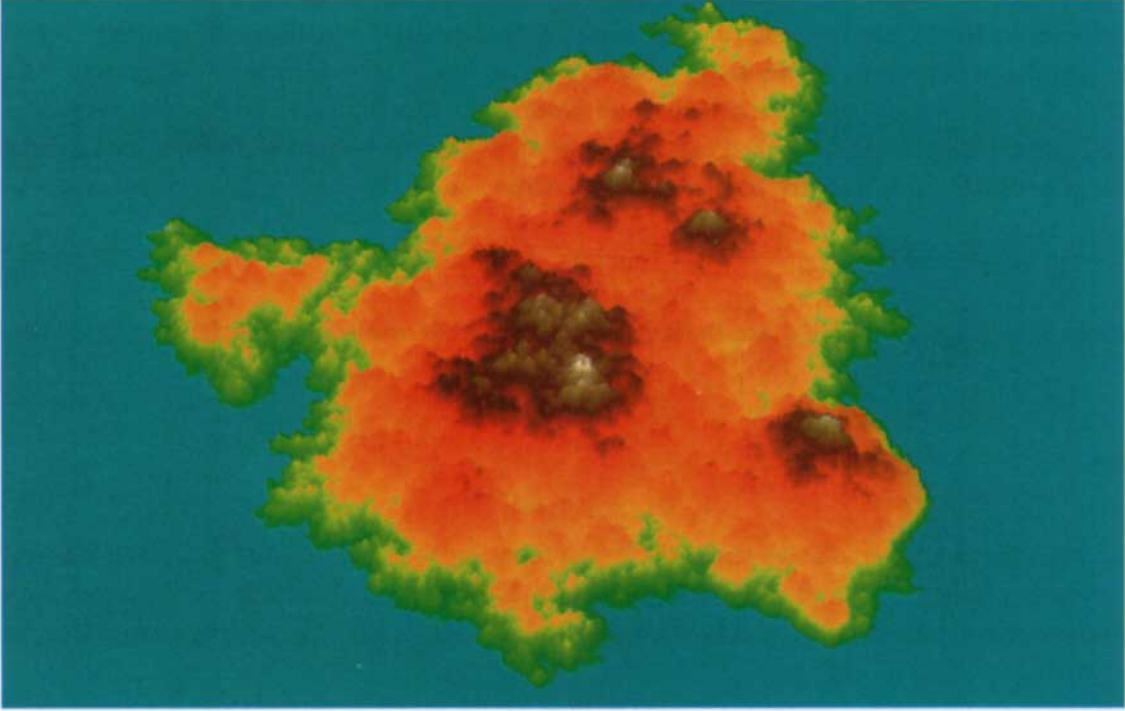


Fig. 1 (a) A three dimensional “airplane” view of a directed surface that completely pinned an avalanche in $(2 + 1)$ dimensions for $p = 0.801$, presented as an island surrounded by a flat “sea”. We used definition B, i.e., the avalanche was started at the center of the figure from the initial flat horizontal surface shown in blue. The Sneppen update rule was used. The diameter of the avalanche is approximately 2^{10} . The uniform blue area shows the region left unchanged since the beginning of the process. The color code for heights corresponds to a conventional color code often used in geographical maps. The white “snow caps” corresponds to the largest heights of the interface. Note that the interfaces of a completely pinned avalanche are the same in the DPD and the SOD models.

Other rules of erosion may be implemented: the bounded slope rule implemented by Tang and Leschhorn,²⁸ or the rule of instantaneously-adjusting slopes introduced by Sneppen.⁵⁰ The DPD model can be introduced on other types of lattices, e.g., on a tilted square or cubical lattice. In this case the DPD model becomes equivalent to the diode-resistor percolation problem introduced more than a decade ago^{58,59}; see also Refs. 17 and 46. The initial condition of the DPD model may be different. One way to start the process is from a single wet cell on a flat interface¹⁷ (see Fig. 1). Another way is to start from a flat interface with periodic boundaries in which each cell is wet.¹⁶

In the SOD model, at each time step all the cells which are in contact with wet cells are examined and the one with the minimal value of η_i is selected and becomes wet. In addition there is a rule of eroding overhangs¹³ or adjusting slopes introduced by Sneppen⁵⁰: all the neighboring cells become wet until all neighboring cells on the interface satisfy a condition that the difference in heights of neighboring points is less than or equal to one. In other words, cells instantaneously become wet if their heights h_i and horizontal coordinates x_{ij} , ($1 \leq j \leq d$) satisfy the inequality:

$$h_i \leq h_0 - \sum_{j=1}^d |x_{ij} - x_{0j}|, \quad (2.1)$$

where h_0 and x_{0j} are coordinates of the cell that becomes wet due to minimal value of η_i .

In the DPD model, the interface is eventually pinned if the value of p is below p_c , where p_c is the critically directed percolation threshold. Otherwise the interface in the infinite system propagates indefinitely. In the DPD model, one can, however, modify a rule of growth¹⁶ and allow the cells whose $\eta_i > p$ (those that are blocked) to erode at an infinitesimal rate. Thus the removal of a random blocked cell produces an avalanche of growth until, once again, all the cells on the interface are blocked. The distribution of the total avalanche volume s is:

$$P(s) \sim s^{-\tau} f\left(\frac{s}{s_c}\right), \quad (2.2)$$

where $s_c \sim \xi_{\parallel}^d \xi_{\perp}$, and ξ_{\parallel} , ξ_{\perp} are horizontal and vertical correlation lengths that scale as:

$$\xi_{\parallel} \sim |p - p_c|^{-\nu_{\parallel}}, \quad (2.3)$$

and

$$\xi_{\perp} \sim |p - p_c|^{-\nu_{\perp}}. \quad (2.4)$$

In analogy with percolation theory,⁶⁰⁻⁶² the function $f(x)$ in Eq. (2.2) is a cutoff function: $f(x) = 1$ when $x \ll 1$ and $f(x) = 0$ when $x \gg 1$. The typical volume of an avalanche s_c diverges when $p \rightarrow p_c$ as $|p - p_c|^{-1/\sigma}$, where $1/\sigma = d\nu_{\parallel} + \nu_{\perp}$. The average avalanche size $\langle s \rangle$ diverges when $p \rightarrow p_c$ as:

$$\langle s \rangle \sim |p - p_c|^{-\gamma}, \quad (2.5)$$

where

$$\gamma = \frac{\tau - 2}{\sigma} = \frac{1}{\sigma} - \beta_p, \quad (2.6)$$

and β_p is an exponent of the order parameter. The physical meaning of the order parameter is the probability for an avalanche to percolate through the characteristic volume s_c . In analogy with percolation $\beta_p = (d - d_c)\nu_{\parallel}$, where d_c is the fractal dimension of points on the interface which can start a percolating avalanche. Using Eq. (2.6) one gets⁶³:

$$\tau = 1 + \frac{d - d_c}{d + \alpha}. \quad (2.7)$$

For length scales smaller than ξ_{\parallel} , the interface is self-affine with roughness exponent of a completely blocked interface:

$$\alpha = \frac{\nu_{\perp}}{\nu_{\parallel}}. \quad (2.8)$$

Another way of generating avalanches in the DPD model is to start every avalanche with a single unblocked cell on a flat surface and wait until the interface is entirely blocked by a directed surface.¹⁷ We will call this definition of the avalanche definition ‘‘B’’ to contrast it with the original avalanche definition¹⁶ described above, which we will refer to as definition A. One may expect that the exponent σ and τ , characterizing the distribution of the avalanches, should be the same for both definitions of the avalanches. However numerical studies of Gat and Olami⁴⁸ showed that $\tau_A < \tau_B$, leading to the inequality $\gamma_A > \gamma_B$. Note that for the Cayley tree model, the exact results of the exponents for definition B are $\nu_{\parallel} = 1/4$ (for $p > p_c$), $\nu_{\parallel} = 3/4$ (for $p < p_c$), $\nu_{\perp} = 0$, $\alpha = 0$, $\tau_B = 2$, $\theta = 0$, $\beta_p = \infty$ and $\gamma_B = 0$.

Definition A appears to be also exactly solvable on the Cayley Tree,⁶⁴ and it yields exponents identical to those in definition B except for γ ; $\gamma_A = 1$. Exponent τ_A is equal to 2 in both cases, but Eq. (2.2) has different logarithmic corrections, thus yielding an average cluster size that diverges in model A ($\gamma_A = 1$) and converges in model B ($\gamma_B = 0$).

The numerical results in high dimensions in avalanche definition A demonstrate that γ_A monotonically approaches 1 from above when dimensionality increases, and for avalanche definition B that $\gamma_B \rightarrow 0$ for $d \rightarrow \infty$. For both definitions, exponents ν_{\parallel} and ν_{\perp} are the same, and in both cases the hyperscaling relation $(d-1)\nu_{\parallel} + \nu_{\perp} = 1/\sigma = \infty$ suggests the same upper critical dimension, $d = \infty$.

In the SOD model, the interface organizes itself to a critical state in which it becomes self-affine on arbitrarily large length scales with the same exponent α . The maximum value of η_i of a cell that has been selected for erosion never exceeds p_c for an infinite system.

It should be pointed out that at any moment of time when the next record η_{\max} of η_i is reached, the interface is the same as it would be in the DPD model in which the value of the driving force equals η_{\max} . In this definition of SOD, no avalanches occur. However, one can artificially define an avalanche as a time span during which the minimum of η_i on the interface is below a certain value p . See also the definition of an associated process in Ref. 52.

The scaling formulae for the avalanche size distribution are the same as in DPD, since the avalanches are bounded by the surfaces of the same geometry. When the avalanche starts or stops, the interface is the same as one of the interfaces that completely stops the growth in the DPD model. One can expect that the exponents τ , ν_{\parallel} , ν_{\perp} , and α are exactly the same in the DPD for definition A and SOD models, since they can be derived from the properties of the same subset of interfaces. Numerical simulations support this point of view.

If one starts the SOD model from a single point on a flat interface, every other cell having the strongest possible value of blocking force $\eta_i = 1$, then the distribution of the first avalanches, i.e., the distribution of the amount of material that becomes wet at the moment when the cell with $\eta_i \geq p$ was removed for the first time, would be the same as in definition B for DPD.

For the SOD model it is possible to derive an additional scaling relation^{52,53}:

$$\gamma_A = 1 + \nu_{\perp}. \quad (2.9)$$

Using Eq. (2.6), one gets:

$$\tau_A = 1 + \frac{d - 1/\nu_{\parallel}}{d + \alpha}. \quad (2.10)$$

Analogous relations are well known for invasion percolation⁶⁵:

$$\tau_A = 1 + \frac{d_h - d_r}{D}, \quad (2.11)$$

where d_h , $d_r = 1/\nu$, and D denotes the fractal dimensions of the hull, the red bonds, and the percolation cluster, respectively. Equations (2.9) and (2.10) seem to be in agreement with numerical simulations in high dimension for definition A of DPD, and with the infinite-dimension limit on the Cayley tree. Comparing relations (2.7) and (2.10), one concludes that for definition A, $d_c = 1/\nu_{\parallel}$. Thus d_c for definition A is analogous to the fractal dimension of the red bonds in percolation.⁶³

For definition B, neither Eq. (2.9) nor Eq. (2.10) is valid. However, for both definitions, τ and γ are still related by Eq. (2.6). Moreover, for both definitions, relation (2.7) is satisfied, but for definition B, d_c is not equal to $1/\nu_{\parallel}$. The same phenomenon is observed for invasion percolation,⁶⁵ where the exponents characterizing the invaded regions analogous to avalanches of definition A are not equal to the exponents of the cluster size distribution

of classical percolation which can be grown from a single wet cell by the Leath algorithm in analogy to definition B. In invasion percolation, this simply means that $d_h - d_r$ is not equal to $d - D$, and thus $\tau = d/D \neq \tau_A$. It is also known⁶⁶ that the exponents τ and γ of a percolation cluster started on the half plane boundary differ from the classical values for clusters started from the bulk. The reason for this discrepancy is the complex self-similar or self-affine structure of the interface from which the avalanches of definition A start to grow. Note that for the Bak-Sneppen model of biological evolution,^{55,56} both definitions of avalanches yield the same exponents, since the properties of the interface in this model do not affect the growth.

3. ACTIVE CELLS AND DYNAMIC EXPONENTS IN THE DPD AND SOD MODELS

In the DPD model, during an avalanche that starts at time $t = 0$, at each time step there is a certain number $n_a(t)$ of “active” columns on the interface that contain unblocked cells on the interface. In the SOD model the active cells are those whose $\eta_i < p$, where p is the value of the first cell removed during a particular avalanche. In order to give time in the SOD model a physical meaning, one must redefine the time interval needed to erode one cell as:

$$dt_p = \frac{1}{n_a}. \quad (3.1)$$

This definition of time is called parallel time t_p .⁵⁵

The number of active columns scales with time t and volume s as:

$$n_a(t) \sim t^\delta \sim s^{d_s}. \quad (3.2)$$

The active columns form a fractal dust with a fractal dimension d_F .

The durations of the avalanches are distributed according to the scaling law:

$$P(t) \sim t^{-\tau_{surv}} f\left(\frac{t}{t_c}\right), \quad (3.3)$$

where $t_c = \xi_{\parallel}^z$.

The dynamical exponents of the avalanches and active cells appear to differ in SOD and DPD models. However, in both classes models, z , δ , d_s , τ , and τ_{surv} are related in the same way. Indeed, the size of avalanches and the time are related as:

$$s \sim \xi_{\parallel}^d \xi_{\perp} \sim \xi_{\parallel}^{d+\alpha} \sim t^{d+\alpha/z}. \quad (3.4)$$

Because $p(s)ds = P(t)dt$, the avalanche distributions are related as:

$$(\tau - 1) \frac{d + \alpha}{z} = (\tau_{surv} - 1). \quad (3.5)$$

In the DPD and SOD models some of the avalanche sites are invaded by oncoming fluid when these sites are active sites on the interface; other sites are occupied due to an erosion rule. It is interesting to note that the number of eroded sites for each invaded site is a fixed, model-dependent constant which does not grow with the total size of an avalanche.⁴⁹ Thus

the total volume of an avalanche is proportional to the sum of all active cells n_a invaded during the avalanche:

$$s \sim \int_0^t n_a(t) dt = \int_0^t t^\delta dt = t^{(d+\alpha)/z} = t^{\delta+1}, \quad (3.6)$$

then:

$$\delta = \frac{d + \alpha}{z} - 1. \quad (3.7)$$

Finally, we can also relate the velocity of the interface to the number of active cells, as defined in Eq. (3.2). The velocity at each instant can be obtained as the number of active cells divided by the size of the parallel projection of the invaded region:

$$v \sim n_a(t)/\xi_{\parallel}^d \sim t^\delta/\xi_{\parallel}^d \sim \xi_{\parallel}^{z\delta-d} \sim f^{-\nu_{\parallel}(z\delta-d)}. \quad (3.8)$$

Comparing with Eq. (1.6), we obtain:

$$\theta = \nu_{\parallel}(d - z\delta). \quad (3.9)$$

The fractal dimension of the live cells is related to the distribution of voids between them, i.e., the distribution of linear sizes of the avalanches. If the probability density used to find the void of length ℓ is equal to $\ell^{-\tau_{\parallel}}$, then:

$$d_F = \tau_{\parallel} - 1. \quad (3.10)$$

If we assume that the number of active points in an avalanche of linear size ℓ scales as ℓ^{d_F} , we conclude that:

$$n_a(t) \sim \ell^{d_F} \sim t^{d_F/z}. \quad (3.11)$$

Hence from Eq. (3.7) we conclude that:

$$d_F = d + \alpha - z. \quad (3.12)$$

Also, since $s \sim \ell^{\alpha+d}$, we have [see Eq. (3.2)]:

$$d_s = d_F/(\alpha + d), \quad (3.13)$$

and

$$(\tau_{\parallel} - 1) = (\tau - 1)(d + \alpha). \quad (3.14)$$

After some algebra, we get⁵⁵:

$$z = (2 - \tau)(d + \alpha). \quad (3.15)$$

However, the assumption $n(t) \sim \ell^{d_F}$ is not necessarily true.

We know that in DPD, z is very close to the chemical dimension of the regular isotropic percolation in d -dimensions.⁶⁷ Thus, in $d = 1$, $z = 1$. However, plugging into Eq. (3.15) the numerical values^{16,52} for $\tau = 1.29$ and $\alpha = 0.63$ in $d = 1$, we get $z = 0.71 \cdot 1.63 = 1.16$. This apparent contradiction happens because in DPD the live cells clump together in blocks within which the density of active cells is constant while the blocks are forming a fractal set. The correlation function $G(r)$ of active cells in DPD undergoes crossover from small slope for small r to large slopes for large (r): $G(r) \sim r^{d_F-d}$. In $d = 1$, using Eqs. (3.10) and (3.14) we get $G(r) \sim r^{2-\tau_{\parallel}} \sim r^{-0.53}$. This is consistent with our numerical calculations of $G(r)$. However, for small r , $G(r)$ is almost constant. Note that the shape of the moving front

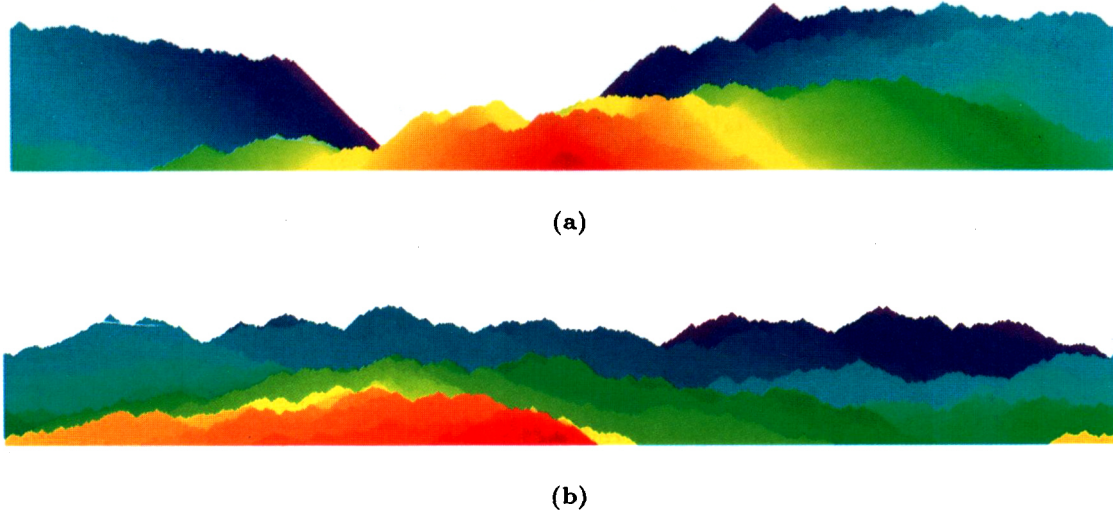


Fig. 2 Illustration of the dynamics of the DPD model at $p = p_c = 0.539$ (a), and the SOD model (b), in $(1+1)$ dimensions. In both cases the Sneppen update rule is used. In both cases the interface is shown after 1000 time steps starting from a single cell near the center on a flat interface (definition B). For the SOD model, the parallel definition of time is used. The “Rainbow” color code indicates time of invasion. Regions invaded at the beginning of the process are displayed in red. The color code changes with time from red to orange, yellow, green, cyan, blue and finally to violet. Note that in DPD model the invasion is caused by lateral propagation of steep slopes that corresponds to constantly changing color in lateral direction. In contrast, in the SOD model the invasion jumps constantly from one part of the interface to the next, that can be seen in part (b) as small alternating “patches” of different colors.

within an avalanche in the SOD model differs from that of the DPD model (see Fig. 2). In the SOD model, the interface is consistently self-affine with the exponent α , and the activity constantly jumps from place to place according to a Lévy flight rule.^{55,56} In the DPD model, the moving interface is not self-affine; it consists of blocked parts interrupted by steep slopes moving as large quasi-particles. Both the horizontal and vertical dimensions of such slopes are of typical size ξ_{\perp} . In $d = 1$ they move with a constant speed $z = 1$. In higher dimensions z is probably equal to the chemical dimension of d -dimensional regular percolation.⁶⁷ In the SOD model, the set of active cells is fractal on all length scales and Eq. (3.11) is correct. Thus it is the self-organization rule — by which we select a site with the smallest value of η_i present in the interface — that causes the value of z in SOD to differ from that of DPD.

To this end, it seems that z cannot be completely determined with the help of only static properties of completely pinned avalanches. In contrast, z depends on the dynamics of active cells that involve the unknown exponent δ [see Eq. (3.7)]. Hence, for any value of δ , one can always satisfy this relation by taking:

$$z = \frac{d + \alpha}{\delta + 1}. \quad (3.16)$$

That is why it is quite possible that in DPD the upper critical dimension is equal to 6 for dynamic exponents⁶⁷ and infinity for static exponents.⁴⁶ (See also Ref. 48 for different interpretation.) The dynamics of the SOD model in which the update rule assumes an infinitely fast propagation of the information along the interface or an infinitesimally slow “creeping”⁶⁸ growth of the interface, differs from the dynamics of KPZ with quenched

disorder and fixed driving force F [see Eq. (1.8)], which is probably in the same universality class as DPD.

ACKNOWLEDGMENTS

We thank O. Gat, Z. Olami, I. Procaccia and R. Zeitak for communicating with us their results prior to publication and helpful contributions and T. Vicsek, G. Huber, B. Sapoval, J. F. Gouyet, M. Paczuski, and H. Leschhorn for valuable discussions. The Center for Polymer Studies is supported by the National Science Foundation. SH acknowledges support from the Israel Science Foundation and JK from OTKA T016568 and the US-Hungarian Joint Fund (contract No. 352).

REFERENCES

1. T. Vicsek, *Fractal Growth Phenomena*, 2nd ed., Part IV (World Scientific, Singapore, 1992); *Dynamics of Fractal Surfaces*, eds. F. Family and T. Vicsek (World Scientific, Singapore, 1991); J. Kertész and T. Vicsek, in *Fractals in Science*, eds. by A. Bunde and S. Havlin (Springer-Verlag, Heidelberg, 1994).
2. J. Krug and H. Spohn, in *Solids Far From Equilibrium: Growth, Morphology and Defects*, edited by C. Godrèche (Cambridge University Press, Cambridge, 1991).
3. P. Meakin, *Phys. Rep.* **235**, 189 (1993).
4. T. Halpin-Healey and Y.-C. Zhang, *Phys. Rep.* **254**, 215 (1995).
5. A.-L. Barabási and H. E. Stanley, *Fractal Concepts in Surface Growth* (Cambridge University Press, Cambridge, 1995).
6. J.-F. Gouyet, M. Rosso and B. Sapoval, in *Fractals and Disordered Systems*, eds. A. Bunde and S. Havlin (Springer-Verlag, Heidelberg, 1991).
7. J. P. Stokes, A. P. Kushnick and M. O. Robbins, *Phys. Rev. Lett.* **60**, 1386 (1988).
8. M. A. Rubio, C. A. Edwards, A. Dougherty and J. P. Gollub, *Phys. Rev. Lett.* **63**, 1685 (1989); V. K. Horváth, F. Family and T. Vicsek, *Ibid.* **65**, 1388 (1990), M. A. Rubio, C. A. Edwards, A. Dougherty and J. P. Gollub, *Ibid.*, 1389 (1990).
9. T. Vicsek, M. Cserző and V. K. Horváth, *Physica* **A167**, 315 (1990).
10. V. K. Horváth, F. Family and T. Vicsek, *J. Phys.* **A24**, L25 (1991); *Phys. Rev. Lett.* **67**, 3207 (1991).
11. S. He, G. L. M. K. S. Kahanda and P.-Z. Wong, *Phys. Rev. Lett.* **69**, 3731 (1992).
12. J. Zhang, Y.-C. Zhang, P. Alstrøm and M. T. Levinsen, *Physica* **A189**, 383 (1992).
13. S. Havlin, A.-L. Barabási, S. V. Buldyrev, C. K. Peng, M. Schwartz, H. E. Stanley and T. Vicsek, in *Growth Patterns in Physical Sciences and Biology* [Proc. 1991 NATO Advanced Research Workshop, Granada], eds. J. M. Garcia-Ruiz, E. Louis, P. Meakin and L. M. Sander (Plenum Press, New York, 1993).
14. S. V. Buldyrev, A.-L. Barabási, S. Havlin, F. Caserta, H. E. Stanley and T. Vicsek, *Phys. Rev.* **A45**, R8313 (1992).
15. S. V. Buldyrev, A.-L. Barabási, S. Havlin, J. Kertész, H. E. Stanley and H. S. Xenias, *Physica* **A191**, 220 (1992).
16. A.-L. Barabási, S. V. Buldyrev, S. Havlin, G. Huber, H. E. Stanley and T. Vicsek, in *Surface Disordering: Growth, Roughening and Phase Transitions*, eds. R. Jullien, J. Kertész, P. Meakin and D. E. Wolf (Nova Science, New York, 1992).
17. S. V. Buldyrev, S. Havlin and H. E. Stanley, *Physica* **A200**, 200 (1993); S. V. Buldyrev, S. Havlin, J. Kertész, A. Shehter and H. E. Stanley, *Fractals* **1**, 827 (1993).
18. L. A. N. Amaral, A.-L. Barabási, S. V. Buldyrev, S. Havlin and H. E. Stanley, *Phys. Rev. Lett.* **72**, 641 (1994); *Fractals* **1**, 818 (1993).
19. F. Family and T. Vicsek, *J. Phys.* **A18**, L75 (1985).
20. F. Family, *J. Phys.* **A19**, L441 (1986).
21. P. Meakin, P. Ramanlal, L. M. Sander and R. C. Ball, *Phys. Rev.* **A34**, 5091 (1986).

22. J. M. Kim and J. M. Kosterlitz, *Phys. Rev. Lett.* **62**, 2289 (1989).
23. S. F. Edwards and D. R. Wilkinson, *Proc. R. Soc. Lond.* **A381**, 17 (1982).
24. M. Kardar, G. Parisi and Y.-C. Zhang, *Phys. Rev. Lett.* **56**, 889 (1986).
25. E. Medina, T. Hwa, M. Kardar and Y.-C. Zhang, *Phys. Rev.* **A39**, 3053 (1989); C. K. Peng, S. Havlin, M. Schwartz and H. E. Stanley, *Phys. Rev.* **A44**, 2239 (1991); J. G. Amar, P.-M. Lam and F. Family, *Phys. Rev.* **A43**, 4548 (1991).
26. Y.-C. Zhang, *J. Physique* **51**, 2129 (1990); S. V. Buldyrev, S. Havlin, J. Kertész, H. E. Stanley and T. Vicsek, *Phys. Rev.* **A43**, 7113 (1991); S. Havlin, S. V. Buldyrev, H. E. Stanley and G. H. Weiss, *J. Phys.* **A24**, L925 (1991).
27. A.-L. Barabási, *Phys. Rev.* **A46**, R2977 (1992).
28. L.-H. Tang and H. Leschhorn, *Phys. Rev.* **A45**, R8309 (1992).
29. V. K. Horváth and H. E. Stanley, "Temporal Scaling of Interfaces Propagating in Porous Media," *Phys. Rev.* **E52**, 5166 (1995).
30. M. Cieplak and M. O. Robbins, *Phys. Rev. Lett.* **60**, 2042 (1988); N. Martys, M. Cieplak and M. O. Robbins, *Phys. Rev. Lett.* **66**, 1058 (1991).
31. C. S. Nolle, B. Koiller, N. Martys and M. O. Robbins, *Phys. Rev. Lett.* **71**, 2074 (1993); B. Koiller, M. O. Robbins, H. Ji and C. S. Nolle, in *New Trends in Magnetic Materials and their Applications*, eds. J. L. Moran-Lopez and J. M. Sanchez (Plenum, New York, 1993).
32. D. A. Kessler, H. Levine and Y. Tu, *Phys. Rev.* **A43**, 4551 (1991).
33. G. Parisi, *Europhys. Lett.* **17**, 673 (1992); L. A. N. Amaral (unpublished).
34. H. Leschhorn, *Physica* **A195**, 324 (1993).
35. M. Dong, M. C. Marchetti, A. A. Middleton and V. Vinokur, *Phys. Rev. Lett.* **70**, 662 (1993).
36. M. Benoit and R. Jullien, *Physica* **A207**, 500 (1994).
37. D. Spasojevic and P. Alstrøm, *Physica* **A201**, 482 (1993).
38. Z. Csahók, K. Honda and T. Vicsek, *J. Phys.* **A26**, L171 (1993); Z. Csahók, K. Honda, E. Somfai, M. Vicsek and T. Vicsek, *Physica* **A200**, 136 (1993).
39. S. Stepanow, *J. Phys. II (France)* **5**, 11 (1995).
40. L. A. N. Amaral, A.-L. Barabási and H. E. Stanley, *Phys. Rev. Lett.* **73**, 62 (1994); L. A. N. Amaral, A.-L. Barabási, H. A. Makse and H. E. Stanley, *Phys. Rev.* **E52**, 4087 (1995).
41. L.-H. Tang, M. Kardar and D. Dhar, *Phys. Rev. Lett.* **74**, 920 (1995).
42. H. A. Makse and L. A. N. Amaral, *Europhys. Lett.* **31**, 379 (1995).
43. T. Nattermann, S. Stepanov, L.-H. Tang and H. Leschhorn, *J. Phys. II (France)* **2**, 1483 (1992); H. Leschhorn, T. Nattermann, S. Stepanov and L.-H. Tang, *Phys. Rev.* **E** (submitted).
44. O. Narayan and D. S. Fisher, *Phys. Rev.* **B48**, 7030 (1993).
45. M. V. Feigel'man, *Sov. Phys. JETP* **58**, 1076 (1983); R. Bruinsma and G. Aeppli, *Phys. Rev. Lett.* **52**, 1547 (1984); J. Koplik and H. Levine, *Phys. Rev.* **B46**, 280 (1985).
46. S. V. Buldyrev, S. Havlin, J. Kertész, R. Sadr-Lahijany, A. Shehter and H. E. Stanley, *Phys. Rev.* **E52**, 373 (1995); see also the application of the Cayley tree to avalanches in lung inflation [A.-L. Barabási, S. V. Buldyrev, H. E. Stanley and B. Suki (preprint)].
47. L. A. N. Amaral, A.-L. Barabási, S. V. Buldyrev, S. Havlin, S. T. Harrington, R. Sadr-Lahijany and H. E. Stanley, *Phys. Rev.* **E51**, 4655 (1995).
48. O. Gat and Z. Olami (unpublished).
49. Z. Olami, I. Procaccia and R. Zeitak, *Phys. Rev.* **E52**, 3402 (1995).
50. K. Sneppen, *Phys. Rev. Lett.* **69**, 3539 (1992); L.-H. Tang and H. Leschhorn, *Ibid.* **70**, 3832 (1993); K. Sneppen and M. H. Jensen, *Ibid.* **70**, 3833 (1993); K. Sneppen and M. H. Jensen, *Phys. Rev. Lett.* **71**, 101 (1993).
51. H. Leschhorn and L.-H. Tang, *Phys. Rev.* **E49**, 1238 (1994).
52. Z. Olami, I. Procaccia and R. Zeitak, *Phys. Rev.* **E49**, 1232 (1994).
53. S. Maslov and M. Paczuski, *Phys. Rev.* **E50**, R643 (1994).
54. P. Bak, C. Tang and K. Wiesenfeld, *Phys. Rev. Lett.* **59**, 381 (1987).
55. P. Bak and K. Sneppen, *Phys. Rev. Lett.* **71**, 4083 (1993); M. Paczuski, S. Maslov and P. Bak, *Europhys. Lett.* **27**, 96 (1994); S. Maslov, M. Paczuski and P. Bak, *Phys. Rev. Lett.* **73**, 2162 (1994); M. Paczuski, P. Bak and S. Maslov, *Phys. Rev. Lett.* **74**, 4253 (1995); M. Paczuski, S. Maslov and P. Bak, *Phys. Rev.* **53**, 414 (1996).
56. T. Ray and N. Jan, *Phys. Rev. Lett.* **72**, 4045 (1994); B. Jovanović, S. V. Buldyrev, S. Havlin and H. E. Stanley, *Phys. Rev.* **E50**, R2403 (1994).
57. B. Suki, A.-L. Barabási, Z. Hantos, F. Peták and H. E. Stanley, *Nature* **368**, 615 (1994).

58. D. Dhar, M. Barma and M. K. Phani, *Phys. Rev. Lett.* **47**, 1238 (1981).
59. S. Redner, *Phys. Rev.* **B25**, 3242 (1982).
60. D. Stauffer and A. Aharony, *Introduction to Percolation Theory*, 2nd ed. (Taylor & Francis, London, 1992).
61. *Fractals and Disordered Systems*, eds. A. Bunde and S. Havlin (Springer-Verlag, Heidelberg, 1991); S. Havlin and D. Ben-Avraham, *Adv. Phys.* **36**, 695 (1987).
62. J. W. Essam, K. De'Bell, J. Adler and F. M. Bhatti, *Phys. Rev.* **B33**, 1982 (1986); J. W. Essam, A. J. Guttmann and K. De'Bell, *J. Phys.* **A21**, 3815 (1988).
63. G. Huber, M. H. Jensen and K. Sneppen, *Phys. Rev.* **E52**, R2133 (1995).
64. S. V. Buldyrev et al. (unpublished).
65. J. F. Gouyet, *Physica* **A168**, 581 (1990).
66. J. L. Cardy, *Nuclear Phys.* **B240**, 514 (1984).
67. S. Havlin, L. A. N. Amaral, S. V. Buldyrev, S. T. Harrington and H. E. Stanley, *Phys. Rev. Lett.* **74**, 4205 (1995).
68. S. I. Zaitsev, *Physica* **A189**, 411 (1992).